Model Complexes for the Active Form of Galactose Oxidase. Physicochemical Properties of Cu(II)− and Zn(II)−Phenoxyl Radical Complexes

Shinobu Itoh,*,† Masayasu Taki,‡ Hideyuki Kumei,‡ Shigehisa Takayama,‡ Shigenori Nagatomo,§ Teizo Kitagawa,*,§ Norio Sakurada,|| Ryuichi Arakawa,*,|| and Shunichi Fukuzumi*,‡

Department of Chemistry, Graduate School of Science, Osaka City University, 3-3-138 Sugimoto, Sumiyoshi-ku, Osaka 558-8585, Japan, Department of Material and Life Science, Graduate School of Engineering, Osaka University, CREST, Japan Science and Technology Corporation, 2-1 Yamada-oka, Suita, Osaka 565-0871, Japan, Institute for Molecular Science, Myodaiji, Okazaki 444-8585, Japan, and Department of Applied Chemistry, Faculty of Engineering, Kansai University, 3-3-35 Yamate-cho, Suita, Osaka 564-8680, Japan

Received August 24, 1999

Introduction

Protein radicals have now been well-recognized to play a crucial role in several biologically important redox processes.[1] Galactose oxidase (GAO, EC 1.1.3.9) is one of the most well-characterized examples of such systems, where a tyrosyl radical directly coordinated to the Cu(II) center is the active species in the aerobic oxidation of D-galactose and primary alcohols to the corresponding aldehydes (eq 1).[2−4] The crystal structure of

$$RCH_2OH + O_2 \rightarrow RCHO + H_2O_2 \qquad (1)$$

galactose oxidase at 1.7 Å resolution has clearly shown that the tyrosine residue (Tyr272, the precursor of the tyrosyl radical) is covalently bound to the sulfur atom of the adjacent Cys228 at the α-position of the phenol ring as illustrated in Chart 1.[2] Recently, such a phenoxyl radical−copper catalytic motif has also been found in glyoxal oxidase (GLO) from *Phanerochaete chrysosporium* and in the prokaryotic FbfB protein.[5,6]

Chart 1

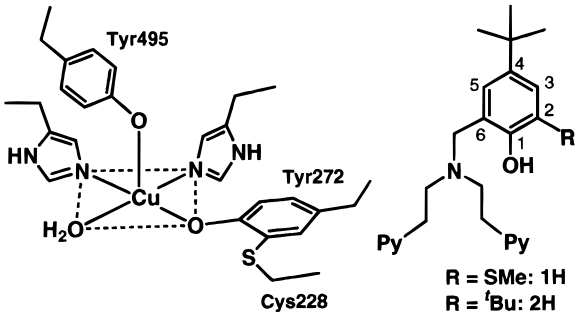

Recent model studies on GAO have provided detailed insights into the physicochemical properties of the phenolate and the phenoxyl radical states of the cofactor both in the metal-free form and in the metal complexes.[7−15] Efficient catalytic reactions for the alcohol oxidation have also been developed by mimicking the enzymatic functions in model systems.[10,11,13] However, few examples have been reported that can reproduce both the spectroscopic characteristics and the chemical functions of the active form of GAO (fully oxidized state). Moreover, little attention has so far been focused on the electronic effects of the thioether group of the cofactor on the physicochemical properties and the reactivity of the Cu(II)−phenoxyl radical species in model systems. In this context, we recently developed a model complex for the active form of GAO using a cofactor-containing ligand **1H**,[16] with which we have successfully demonstrated the important role of the copper ion in the efficient two-electron oxidation of alcohols.[17] In this paper, we report detailed characterizations of the Cu(II)- and Zn(II)−phenoxyl

† Osaka City University.
‡ Osaka University.
§ Institute for Molecular Science.
|| Kansai University.

(1) Stubbe, J.; van der Donk, W. A. *Chem. Rev.* **1998**, *98*, 705 and references therein.
(2) (a) Ito, N.; Phillips, S. E. V.; Stevens, C.; Ogel, Z. B.; McPherson, M. J.; Keen, J. N.; Yadav, K. D. S.; Knowles, P. F. *Nature* **1991**, *350*, 87. (b) Ito, N.; Phillips, S. E. V.; Yadav, K. D. S.; Knowles, P. F. *J. Mol. Biol.* **1994**, *238*, 794.
(3) (a) Whittaker, M. M.; Whittaker, J. W. *J. Biol. Chem.* **1988**, *263*, 6074. (b) Whittaker, M. M.; DeVito, V. L.; Asher, S. A.; Whittaker, J. W. *J. Biol. Chem.* **1989**, *264*, 7104. (c) Whittaker, M. M.; Whittaker, J. W. *J. Biol. Chem.* **1990**, *265*, 9610. (d) Whittaker, M. M.; Whittaker, J. W. *Biophys. J.* **1993**, *64*, 762. (e) Whittaker, M. M.; Ballou, D. P.; Whittaker, J. W. *Biochemistry* **1998**, *37*, 8426.
(4) (a) Branchaud, B. P.; Montague-Smith, M. P.; Kosman, D. J.; McLaren, F. R. *J. Am. Chem. Soc.* **1993**, *115*, 798. (b) Wachter, R. M.; Branchaud, B. P. *Biochemistry* **1996**, *35*, 14425. (c) Wachter, R. M.; Montague-Smith, M. P.; Branchaud, B. P. *J. Am. Chem. Soc.* **1997**, *119*, 7743.
(5) (a) Kersten, P. J. *Proc. Natl. Acad. Sci. U.S.A.* **1990**, *87*, 2936. (b) Whittaker, M. M.; Kersten, P. J.; Nakamura, N.; Sanders-Loehr, J.; Schweizer, E. S.; Whittaker, J. W. *J. Biol. Chem.* **1996**, *271*, 681.
(6) Bork, P.; Doolittle, R. F. *J. Mol. Biol.* **1994**, *236*, 1277.
(7) (a) Itoh, S.; Hirano, K.; Furuta, A.; Komatsu, M.; Ohshiro, Y.; Ishida, A.; Takamuku, S.; Kohzuma, T.; Nakamura, N.; Suzuki, S. *Chem. Lett.* **1993**, 2099. (b) Itoh, S.; Takayama, S.; Arakawa, R.; Furuta, A.; Komatsu, M.; Ishida, A.; Takamuku, S.; Fukuzumi, S. *Inorg. Chem.* **1997**, *36*, 1407.
(8) (a) Whittaker, M. M.; Chuang, Y.-Y.; Whittaker, J. W. *J. Am. Chem. Soc.* **1993**, *115*, 10029. (b) Whittaker, M. M.; Duncan, W. R.; Whittaker, J. W. *Inorg. Chem.* **1996**, *35*, 382.
(9) (a) Halfen, J. A.; Young, V. G., Jr.; Tolman, W. B. *Angew. Chem.* **1996**, *108*, 1832; *Angew. Chem., Int. Ed. Engl.* **1996**, *108*, 1832. (b) Halfen, J. A.; Jazdzewski, B. A.; Mahapatra, S.; Berreau, L. M.; Wilkinson, E. C.; Que, L., Jr.; Tolman, W. B. *J. Am. Chem. Soc.* **1997**, *119*, 8217.
(10) Kitajima, N.; Whang, K.; Moro-oka, Y.; Uchida, A.; Sasada, Y. *J. Chem. Soc., Chem. Commun.* **1986**, 1504.
(11) (a) Wang, Y.; Stack, T. D. P. *J. Am. Chem. Soc.* **1996**, *118*, 13097. (b) Wang, Y.; DuBois, J. L.; Hedman, B.; Hodgson, K. O.; Stack, T. D. P. *Science* **1998**, *279*, 537.
(12) Sokolowski, A.; Müller, J.; Weyhermüller, T.; Schnepf, R.; Hildebrandt, P.; Hildenbrand, K.; Bothe, E.; Wieghardt, K. *J. Am. Chem. Soc.* **1997**, *119*, 8889.
(13) (a) Chaudhuri, P.; Hess, M.; Flörke, U.; Wieghardt, K. *Angew. Chem.* **1998**, *110*, 2340; *Angew. Chem., Int. Ed. Engl.* **1998**, *37*, 2217. (b) Chaudhuri, P.; Hess, M.; Weyhermüller, T.; Wieghardt, K. *Angew. Chem.* **1999**, *111*, 1165; *Angew. Chem., Int. Ed. Engl.* **1999**, *38*, 1095. (c) Chaudhuri, P.; Hess, M.; Müller, J.; Hildenbrand, K.; Bill, E.; Weyhermüller, T.; Wieghardt, K. *J. Am. Chem. Soc.* **1999**, *121*, 9599.
(14) Ruf, M.; Pierpont, C. G. *Angew. Chem.* **1998**, *110*, 1830; *Angew. Chem., Int. Ed. Engl.* **1998**, *37*, 1736.
(15) (a) Halcolm, M. A.; Chia, L. M. L.; Liu, X.; McInnes, E. J. L.; Yellowlees, L. J.; Mabbs, F. E.; Davies, J. E. *Chem. Commun.* **1998**, 2465. (b) Halcolm, M. A.; Chia, L. M. L.; Liu, X.; McInnes, E. J. L.; Yellowlees, L. J.; Mabbs, F. E.; Scowen, I. J.; McPartlin, M.; Davies, J. E. *J. Chem. Soc., Dalton Trans.* **1999**, 1753.
(16) To distinguish the different states of the cofactor moiety of the ligands more clearly, the symbols of **LH**, $\mathbf{L}^-$, and $\mathbf{L}^{\bullet}$ (**L** = **1** or **2**) are used to denote the phenol, phenolate, and phenoxyl radical forms, respectively.

10.1021/ic9910211 CCC: $19.00
Published on Web 07/13/2000

radical complexes of ligand **1H** as well as of its 2,4-di-*tert*-butyl derivative **2H**[16] as a reference to shed light on the role of the thioether group of the cofactor.

Results and Discussion

Ligand **1H** was prepared from 4-*tert*-butylphenol by acid-catalyzed sulfenylation with dimethyl disulfide followed by a Mannich reaction with bis[2-(2-pyridyl)ethyl]amine and paraformaldehyde as employed for the synthesis of the 4-methyl derivative of **1H**.[7b] Another ligand **2H** was obtained in one step by the Mannich reaction of 2,4-di-*tert*-butylphenol, paraformaldehyde, and bis[2-(2-pyridyl)ethyl]amine. Treatment of the deprotonated ligand $\mathbf{1}^-$ [16] with $CuCl_2$ in methanol led to the formation of a copper(II) complex that immediately crystallized as a dimer, $[Cu^{II}_2(\mathbf{1}^-)_2](PF_6)_2$, when $NaPF_6$ was added to the solution.[18] The Zn(II) complex of $\mathbf{1}^-$ was also isolated as a dimer, $[Zn^{II}_2(\mathbf{1}^-)_2](PF_6)_2$, in a similar manner using $Zn(ClO_4)_2 \cdot 6H_2O$ instead of $CuCl_2$.[18] These dimeric Cu(II) and Zn(II) complexes of $\mathbf{1}^-$ can be converted into the corresponding monomeric complexes, $[Cu^{II}(\mathbf{1}^-)(AcO^-)]$ and $[Zn^{II}(\mathbf{1}^-)(CH_3CN)]PF_6$, in CH_3CN by the coordination of the external ligand (AcO^-) and the solvent, respectively.[18] In contrast to the case of ligand $\mathbf{1}^-$, the Cu(II) and Zn(II) complexes of ligand **2H** were isolated as mononuclear complexes, $[Cu^{II}(\mathbf{2}^-)(CH_3CN)]PF_6$ and $[Zn^{II}(\mathbf{2}^-)(CH_3CN)]PF_6$, when the deprotonated ligand $\mathbf{2}^-$ [16] was treated with $CuCl_2$ and $Zn(ClO_4)_2 \cdot 6H_2O$, respectively, in CH_3OH followed by the addition of $NaPF_6$.[18] All mononuclear phenolate complexes, $[Cu^{II}(\mathbf{1}^-)(AcO^-)]$, $[Zn^{II}(\mathbf{1}^-)(CH_3CN)]PF_6$, $[Cu^{II}(\mathbf{2}^-)(CH_3CN)]PF_6$, and $[Zn^{II}(\mathbf{2}^-)(CH_3CN)]PF_6$, exhibited a reversible redox couple for the one-electron oxidation of the phenolate at 0.14, 0.51, 0.44, and 0.50 V vs $Ag/AgNO_3$, respectively.[18] The large difference in redox potential between the first complex and the other three could be attributed mainly to the difference in the external ligand: AcO^- vs CH_3CN.

Figure 1A shows the spectral changes observed upon addition of an equimolar amount of $(NH_4)_2[Ce^{IV}(NO_3)_6]$ (CAN) per copper ion to a CH_3CN solution of $[Cu^{II}_2(\mathbf{1}^-)_2](PF_6)_2$ (2.5×10^{-4} M), where the absorption band at 522 nm due to the phenolate complex immediately disappears together with the concomitant appearance of new absorption bands at 415 nm (ϵ = 1790 M^{-1} cm^{-1}) and 867 nm (550 M^{-1} cm^{-1}) at 25 °C. A similar spectrum is obtained upon the oxidation of $[Zn^{II}(\mathbf{1}^-)(CH_3CN)]PF_6$ by CAN under the same experimental conditions, as shown in Figure 1B [418 nm (1250 M^{-1} cm^{-1}) and 887 nm (510 M^{-1} cm^{-1}) in CH_3CN at 25 °C]. The resulting spectra are very similar in shape to those of the phenoxyl radical species of 2-(methylthio)-*p*-cresol (λ_{max} = 400 and 830 nm)[7,8a] and of the active forms of GAO [444 nm (5194 M^{-1} cm^{-1}) and 800 nm (3211 M^{-1} cm^{-1})] and GLO [448 nm (5700 M^{-1} cm^{-1}) and 851 nm (4300 M^{-1} cm^{-1})],[5b] indicating that the characteristic absorption bands obtained upon the Ce^{IV} oxidation are due to the phenoxyl radical species ($\mathbf{1}^\bullet$)[16] of the ligand. The Cu(II) and Zn(II) complexes of $\mathbf{2}^\bullet$ [16] can also be generated by Ce^{IV} oxidation of the corresponding phenolate compounds. The phenoxyl radical complexes display two characteristic absorption bands around 410 and 670 nm [411 nm (2440 M^{-1} cm^{-1}) and 675 nm (300 M^{-1} cm^{-1}) for the Cu(II) complex and 409 nm (2430 M^{-1} cm^{-1}) and 666 nm (140 M^{-1} cm^{-1}) for the Zn(II) complex; see Figures S12 and S13 in the Supporting Information]. It is interesting to note that both Cu(II) and Zn(II) complexes of the phenoxyl radical $\mathbf{1}^\bullet$ exhibit very broad and strong absorption bands above 850 nm (λ_{max} = 867 and 887 nm), while those of $\mathbf{2}^\bullet$ and of the other phenoxyl radical species thus far reported do not show such characteristic absorption bands above 800 nm,[9,11,12,13a,b] except for one example recently reported by Halcolm et al.[15] On the basis of the spectroscopic and theoretical examinations of the metal-free phenoxyl radical species of cofactor model compounds, we have attributed the broad absorbance above 800 nm to the intramolecular charge transfer from the benzene ring to the methylthio group in the phenoxyl radical group.[7] The larger ϵ values ($\sim$5000 M^{-1} cm^{-1}) of the lower energy absorption bands of GAO and GLO as compared to those of our model compounds (ϵ = $\sim$500 M^{-1} cm^{-1}) may indicate that an interligand charge transfer from Tyr272$^\bullet$ to Tyr495$^-$ also contributes to the characteristic UV−NIR features of the enzymes as suggested by Whittaker et al.[19]

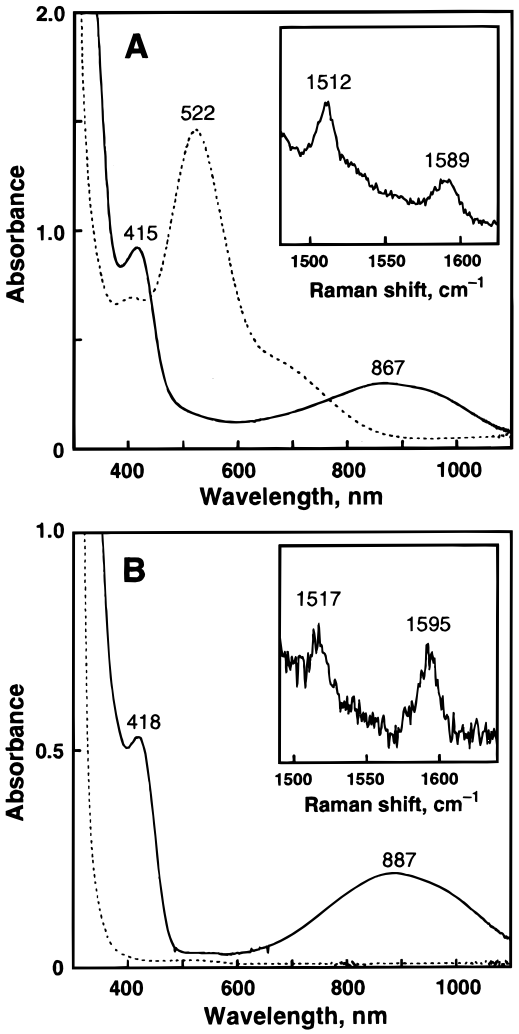

Figure 1. (A) UV−vis spectra of $[Cu^{II}_2(\mathbf{1}^-)_2](PF_6)_2$ (dotted line) (2.5×10^{-4} M) and $[Cu^{II}(\mathbf{1}^\bullet)(NO_3)]^+$ (solid line) in CH_3CN at 25 °C. Inset: Resonance Raman spectrum of $[Cu^{II}(\mathbf{1}^\bullet)(NO_3)]^+$ in CH_3CN at −30 °C. (B) UV−vis spectra of $[Zn^{II}(\mathbf{1}^-)(CH_3CN)](PF_6)_2$ (dotted line) (5.0×10^{-4} M) and $[Zn^{II}(\mathbf{1}^\bullet)(NO_3)]^+$ (solid line) in CH_3CN at 25 °C. Inset: Resonance Raman spectrum of $[Zn^{II}(\mathbf{1}^\bullet)(NO_3)]^+$ in CH_3CN at −30 °C.

(17) Itoh, S.; Taki, M.; Takayama, S.; Nagatomo, S.; Kitagawa, T.; Sakurada, N.; Arakawa, R.; Fukuzumi, S. *Angew. Chem.* **1999**, *111*, 2944; *Angew. Chem., Int. Ed. Engl.* **1999**, *38*, 2774.

(18) Details of the synthetic procedures, X-ray structure determinations, and spectroscopic and electrochemical characterizations for the phenolate complexes are provided in the Supporting Information.

(19) McGlashen, M. L.; Eads, D. D.; Spiro, T. G.; Whittaker, J. W. *J. Phys. Chem.* **1995**, *99*, 4918.

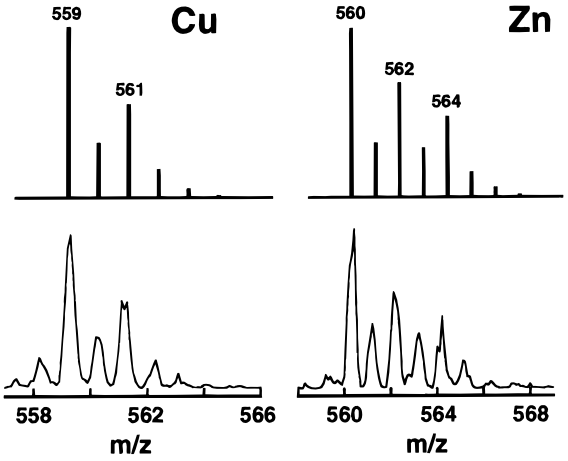

Figure 2. Experimental (bottom) and calculated (top) peak envelopes in the positive-ion electrospray mass spectra of $[Cu^{II}(\mathbf{1}^{\bullet})(NO_3)]^+$ (left) and $[Zn^{II}(\mathbf{1}^{\bullet})(NO_3)]^+$ (right) in CH_3CN.

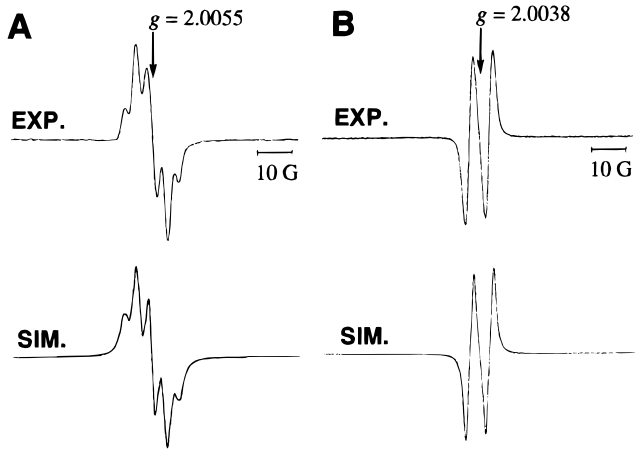

Figure 3. (A) Solution ESR spectrum (EXP) of $[Zn^{II}(\mathbf{1}^{\bullet})(NO_3)]^+$ in CH_3CH_2CN at −80 °C (microwave frequency 9.213 GHz, modulation frequency 100 kHz, modulation amplitude 0.5 G, microwave power 5 mW) and its computer simulation spectrum (SIM). (B) Solution ESR spectrum (EXP) of $[Zn^{II}(\mathbf{2}^{\bullet})(NO_3)]^+$ in CH_3CH_2CN at −80 °C (microwave frequency 9.210 GHz, modulation frequency 100 kHz, modulation amplitude 0.63 G, microwave power 5 mW) and its computer simulation spectrum (SIM).

Formation of the M(II)−phenoxyl radical species was confirmed by resonance Raman spectroscopy (RR; insets of Figure 1), electrospray ionization mass spectroscopy (ESI-MS; Figure 2), and ESR spectroscopy (Figure 3) of the solutions resulting from the Ce^{IV} oxidation of $[Cu^{II}_2(\mathbf{1}^-)_2](PF_6)_2$ and $[Zn^{II}(\mathbf{1}^-)(CH_3CN)]PF_6$. In the RR spectra, both Cu(II) and Zn(II) complexes of $\mathbf{1}^{\bullet}$ display two prominent peaks at 1512 and 1589 cm^{-1} and at 1517 and 1595 cm^{-1}, respectively, which are characteristic vibrational peaks of metal-coordinated phenoxyl radicals[9b,12,20] and of activated GAO (1487, 1595 cm^{-1})[5b] and GLO (1486, 1591 cm^{-1}).[5b] These two bands have been assigned to the modes ν_{7a}' and ν_{8a}', which predominantly include C−O stretching and $C_{ortho}-C_{meta}$ stretching, respectively.[20] The higher energy of the C−O stretching of the phenoxyl radical (ν_{7a}') as compared to that of phenolate ($\nu_{7a} \sim 1250$ cm^{-1})[9b] clearly indicates that the C−O bond of the phenoxyl radical species has a partial double bond character, as we have already suggested on basis of the results of ESR measurements and theoretical calculations.[7] The ESI-MS spectra in Figure 2 each exhibit only a set of prominent peaks with a mass and an isotope distribution pattern being consistent with Cu(II) and the Zn(II) complexes of the phenoxyl radical with one nitrate ion as a coordinated counteranion coming from CAN: $[Cu^{II}(\mathbf{1}^{\bullet})(NO_3)]^+$ and $[Zn^{II}(\mathbf{1}^{\bullet})(NO_3)]^+$.

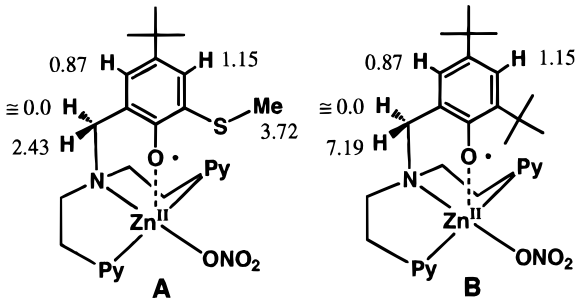

Figure 4. Hyperfine coupling constants (G) determined from the computer simulations for (A) $[Zn^{II}(\mathbf{1}^{\bullet})(NO_3)]^+$ and (B) $[Zn^{II}(\mathbf{2}^{\bullet})(NO_3)]^+$.

A CH_3CN solution of $[Cu^{II}(\mathbf{1}^{\bullet})(NO_3)]^+$ was ESR silent at 77 K, which is consistent with magnetic coupling between the $S = {}^1/_2$ Cu(II) ion and the $S = {}^1/_2$ phenoxyl radical, although the type of coupling (antiferromagnetic or ferromagnetic) is unclear at present. In contrast, the solution ESR spectrum of $[Zn^{II}(\mathbf{1}^{\bullet})(NO_3)]^+$ recorded at −80 °C in C_2H_5CN (Figure 3A) exhibits a well-resolved isotropic signal at $g = 2.0052$, which is very close to those of the cofactor radical (2.0055) in the enzyme active site and of the phenoxyl radicals derived from our cofactor model compounds (2.0052−2.0060).[3c,7b] $[Zn^{II}(\mathbf{2}^{\bullet})(NO_3)]^+$ also affords a well-resolved ESR signal at $g = 2.0038$ under the same experimental conditions (Figure 3B). Hyperfine coupling constants (hfc's) determined from the computer simulations for $[Zn^{II}(\mathbf{1}^{\bullet})(NO_3)]^+$ and $[Zn^{II}(\mathbf{2}^{\bullet})(NO_3)]^+$ (SIMs in Figure 3) are indicated in Figure 4 (parts A and B, respectively). It is obvious that the spin density at the benzylic methylene group in $\mathbf{1}^{\bullet}$ ($a_H = 2.43$ G) is significantly small as compared to that of $\mathbf{2}^{\bullet}$ ($a_H = 7.19$ G), whereas a relatively large amount of the spin delocalizes into the methylthio group in $\mathbf{1}^{\bullet}$ ($a_{Me} = 3.72$ G). The spin delocalization into the methylthio group in $\mathbf{1}^{\bullet}$ is reflected by the larger g value of $[Zn^{II}(\mathbf{1}^{\bullet})(NO_3)]^+$ ($g = 2.0052$) due to the large spin−orbit coupling on the sulfur atom as compared to that of $[Zn^{II}(\mathbf{2}^{\bullet})(NO_3)]^+$ ($g = 2.0038$).

It has been reported that hfc values for benzylic methylene protons of phenoxyl radicals can be estimated by the angle-dependent McConnell-type relationship $a_{C-H} = \rho_{C1}B\cos^2\theta$, where a_{C-H} is the hfc of the methylene proton, ρ_{C1} is the spin density at the C1 position, B is a constant equal to 162 Hz, and θ is the dihedral angle defined in Figure 8 of Babcock's paper.[21] Thus, the ratio of the hfc values of two methylene protons (a_{H1}/a_{H2}) is proportional to $\cos^2\theta_1/\cos^2\theta_2$. If one accepts an assumption that the dihedral angles of benzylic methylene protons do not change upon one-electron oxidation, the a_{H1}/a_{H2} ratio can be calculated as 136 by using the dihedral angles obtained in the X-ray structure of $[Zn^{II}_2(\mathbf{1}^-)_2](PF_6)_2$ ($\theta_{1(av)} = 25.1°$, $\theta_{2(av)} = 85.6°$).[18] Such a large value of a_{H1}/a_{H2} is consistent with the large difference between a_{H1} and a_{H2} (2.43 mT vs ∼0 mT) determined from the computer simulation of the ESR spectrum (Figure 3). Such a good correlation for a_{H1}/a_{H2} indicates the validity of our assumption, suggesting that the phenoxyl radical remains metal-bound. The existence of strong

(20) Schnepf, R.; Sokolowski, A.; Müller, J.; Bachler, V.; Wieghardt, K.; Hildebrandt, P. *J. Am. Chem. Soc*. **1998**, *120*, 2352.

(21) Babcock, G. T.; El-Deeb, M. K.; Sandusky, P. O.; Whittaker, M. M.; Whittaker, J. W. *J. Am. Chem. Soc.* **1992**, *114*, 3727.

magnetic coupling in the Cu(II)−phenoxyl radical species also indicates that there is a direct metal−phenoxyl radical interaction.

In summary, one-electron oxidations of the Cu(II)− and Zn(II)−phenolate complexes of ligand **1H** afford relatively stable phenoxyl radical complexes, which exhibit very characteristic UV−NIR features similar to those exhibited by the active forms of the native enzymes. Comparison of the spectroscopic characteristics (UV−vis and ESR) of the Cu(II) and Zn(II) complexes of **1**• to those of the corresponding complexes of **2**• indicates that the methylthio group of **1**• exerts an electron-sharing conjugative effect, thus stabilizing the radical form of the cofactor, as has been demonstrated in model studies of the metal-free radicals.[7] Such an important role for the thioether group (electron-sharing conjugative effect) has also been predicted by ab initio theory and demonstrated by high-frequency ESR studies of model radicals.[22] It should be noted, however, that such an electronic effect of an alkylthio group is not always observed in other model systems,[9,11,13a] suggesting that the molecular geometry of a complex is also very important to the enhancement of this effect. The smaller ϵ values for the NIR features of the model complexes as compared to those for the active forms of the native enzymes may indicate a strong contribution from Tyr272• → Tyr495$^-$ interligand charge transfer in addition to intramolecular charge transfer from the benzene ring to the alkylthio group in the phenoxyl radical group itself in the enzymatic systems.

Experimental Section

General Procedures. Syntheses of the ligands and the complexes were performed similarly to those reported previously.[7b,18] UV−vis spectra were recorded on a Hewlett-Packard 8452A or a Hewlett-Packard 8453 photodiode array spectrophotometer. ESR spectra were recorded on a JEOL JES-ME-2X spectrometer, and the *g* values were determined using an Mn^{II} marker as a reference. Computer simulations of the ESR spectra were carried out by using ESRaII version 1.01 (Calleo Scientific Publishing Co.) on a Macintosh personal computer. Electrospray ionization mass spectroscopy (ESI-MS) and electrochemical measurements were performed as reported previously.[7b,18]

Visible Resonance Raman Measurements. The 413.1 nm line of a Kr^+ laser (model 2060, Spectra Physics) was used as the exciting source. Visible resonance Raman scattering was measured with a CCD detector (model CCD3200, Astromed) attached to a 1 m single polychromator (model MC-100DG, Ritsu Oyo Kogaku). The slit width and slit height were set to 200 μm and 10 mm, respectively. Wavenumber ranges per channel were 0.9 (Kr^+ laser) and 0.5 cm^{-1} (dye laser). The laser power used was 2.5 mW at the sample point. All measurements were carried out at −40 °C with a spinning cell (1000 rpm). Raman shifts were calibrated with indene, and the accuracy of the peak positions of the Raman bands was ±1 cm^{-1}.

Acknowledgment. This study was financially supported in part by a Grant-in-Aid for Scientific Research on Priority Areas (Molecular Biometallics, Electrochemistry of Ordered Interfaces, and Creation of Delocalized Conjugated Electronic Systems) from the Ministry of Education, Science, Sports, and Culture of Japan and by a Research Fellowship from the Japan Society for the Promotion of Science for Young Scientists (No. 02410).

Supporting Information Available: Textual details of the synthetic procedures, X-ray structure determinations, and spectroscopic and electrochemical characterizations, tables of X-ray experimental details, bond distances, and bond angles, figures showing ORTEP diagrams, UV−vis, EI-MS, and ESR spectra, and cyclic voltammograms (Figures S1−S11), and X-ray crystallographic files, in CIF format, for the phenolate complexes and UV−vis spectra for the Cu(II) and Zn(II) complexes of **2**• (Figures S12 and S13). This material is available free of charge via the Internet at http://pubs.acs.org.

IC9910211

(22) Gerfen, G. J.; Bellew, B. F.; Griffin, R. G.; Singel, D. J.; Ekberg, C. A.; Whittaker, J. W. *J. Phys. Chem.* **1996**, *100*, 16739.